ACS NANO
Cite This: ACS Nano 2018, 12, 9495−9503
www.acsnano.org

ARTICLE

Highly Conducting Hybrid Silver-Nanowire-Embedded Poly(3,4-ethylenedioxythiophene):Poly(styrenesulfonate) for High-Efficiency Planar Silicon/Organic Heterojunction Solar Cells

Joseph P. Thomas, Md Anisur Rahman, Saurabh Srivastava, Jung-Soo Kang, Donald McGillivray, Marwa Abd-Ellah, Nina F. Heinig, and Kam Tong Leung*

WATLab and Department of Chemistry, University of Waterloo, Waterloo, Ontario N2L3G1, Canada

Supporting Information

ABSTRACT: Embedding nanowires, such as silver nanowires (AgNWs), in a transparent conductive polymer poly(3,4-ethylenedioxythiophene):poly(styrenesulfonate) (PEDOT:PSS) to enhance its conductivity is technologically important for improving the performances of devices comprising transparent conductive layers. Addition of nanowires in the highly conducting form of cosolvent (ethylene glycol) or mixed-cosolvent (ethylene glycol and methanol) modified PEDOT:PSS could change the nanowire structure and significantly alter the conductivity. Here, we report a simple method to embed AgNWs in PEDOT:PSS efficiently to improve its conductivity. By incorporating nanowires in the mixed cosolvent matrix prior to addition into PEDOT:PSS, this method preserves the structure of the nanowires while enabling conductivity enhancement. In contrast, the addition of AgNWs into cosolvent-premodified PEDOT:PSS leads to breaking of nanowires and conductivity impediment. The hybrid films with efficiently embedded AgNWs and mixed-cosolvent-modified PEDOT:PSS show a sheet resistance of 104 Ω/□, which is among the lowest ever reported for the as-deposited films, with conductivity enhancement of 33% relative to that of mixed-cosolvent-modified PEDOT:PSS. The resulting planar heterojunction solar cell (HSC) based on AgNW-embedded PEDOT:PSS exhibits a power conversion efficiency of greater than 15%. This demonstrates the importance of reducing sheet resistance by integrating nanowires into the PEDOT:PSS matrix as effective charge-transfer conduits interconnecting the highly conducting quinoid chains. The present approach to efficiently embed AgNWs in PEDOT:PSS could be readily extended to other nanowires or nanoparticles for improving the performance of PEDOT:PSS for applications in not just HSCs but indeed other electronic devices that require both transparent and highly conductive layers.

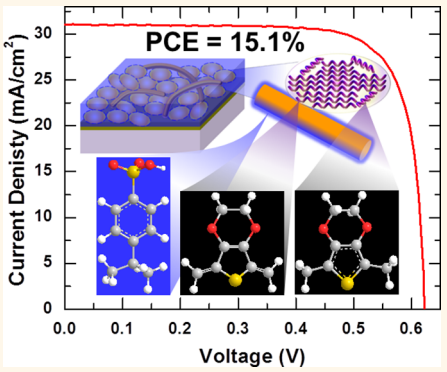

KEYWORDS: *conducting polymer, poly(3,4-ethylenedioxythiophene):poly(styrenesulfonate), PEDOT:PSS, silver nanowire, charge transfer, heterojunction solar cell*

The highly conducting polymer poly(3,4-ethylenedioxythiophene):poly(styrenesulfonate) (PEDOT:PSS) has found many applications as a transparent conducting layer in organic and organic−inorganic electronic devices.[1−5] The aqueous nature of the PEDOT:PSS solution and the simple fabrication processes, such as spin-coating, allow the formation of uniform and homogeneous thin films, making PEDOT:PSS highly attractive for low-cost device fabrication. Several methods to improve the conductivity of PEDOT:PSS have been reported, and they mainly involve the addition of cosolvents[6−8] and surfactants[9−11] to modify its microstructure in the solution phase or the removal of the insulating PSS by post-treatments[5,12−15] of the films. Addition of cosolvents is generally more attractive than post-treatments because certain post-treatment processes, such as acid treatment,[15] often increase the complexities (and therefore the cost) in the device fabrication process. Recently, we reported that the addition of mixed cosolvents [ethylene glycol (EG) and methanol] to PEDOT:PSS can lower the sheet

Received: June 26, 2018
Accepted: August 27, 2018
Published: August 27, 2018

DOI: 10.1021/acsnano.8b04848
ACS Nano 2018, 12, 9495−9503

resistance and improve the conductivity to a greater extent than the addition of a single commonly used cosolvent: EG or dimethylsulfoxide.[6,8] Typically, the cosolvent or mixed cosolvent addition to a PEDOT:PSS solution enhances the conductivity of PEDOT:PSS by facilitating the formation of PEDOT microstructured grains with quinoid chains rather than its less conducting benzoid counterparts.[16−19]

Even though PEDOT:PSS films show high conductivities as a polymer film, improvement in their conductivity by using simple and low-cost methods to outperform the commonly used transparent conducting oxides (TCOs), such as indium tin oxide (ITO), is essential for PEDOT:PSS to become a viable lower-cost alternative to TCOs.[20] In order to achieve higher conductivities, hybrid films that incorporate inorganic nanowires into PEDOT:PSS have attracted much recent attention.[21−24] Among the different choices of nanowires, silver nanowires (AgNWs) are widely used because of their highly conducting nature, flexibility, easy preparation, and commercial availability.[21−23] However, these nanowires have also shown junction resistance that can be detrimental to improving the conductivity.[21] Enhancement in the conductivity of the hybrid AgNWs and PEDOT:PSS combination has been reported, and this was achieved by incorporating nanowires on top or inside PEDOT:PSS layers to produce a conductive layered hybrid film.[21−23] Any successful simple preparation technique for embedding nanowires in a PEDOT:PSS solution to obtain a conductivity higher than that of the cosolvent-modified PEDOT:PSS is highly desirable because of the widespread application of PEDOT:PSS in the fabrication of a wide variety of electronic devices, including all organic or organic−inorganic heterojunction solar cells (HSCs) and flexible electronic devices.

HSCs made of PEDOT:PSS and Si substrates have been recently reported to show very high efficiencies greater than 15%.[25,26] Most of these high-efficiency devices have, however, been fabricated with complex device processing, such as surface texturing of Si substrates[25−30] or a back-junction method involving PEDOT:PSS back-coating.[31] For planar HSCs (involving planar and not surface-textured substrates), efficiencies up to 14−15% could only be achieved by introducing antireflective coatings,[4,32] optimizing PEDOT:PSS properties,[8] and interface engineering by tuning the contact properties of silicon substrates.[26] High-efficiency HSCs that can be produced on planar Si substrates without any complex device fabrication steps are therefore of special interest to reducing the manufacturing cost. Furthermore, simple and effective approaches for incorporating AgNWs in PEDOT:PSS can be beneficial to improve not only the conducting properties but also the solar cell properties because of the scattering and plasmonic effects of nanowires. Although nanowire-coated HSCs involving spin-coated[21] or drop-casted[24] AgNWs on top of a PEDOT:PSS layer have been reported, their efficiencies were only 10−11%. Significant improvement in the efficiency of planar HSCs by incorporating embedded NWs by other methods at least to the present optimal level of 14−15% should be possible and be pursued, given their tremendous commercial potential of low-cost photovoltaic applications.

In the present work, we show that embedding AgNWs after the cosolvent modification of PEDOT:PSS is detrimental, leading to degradation of the AgNWs and reduction in the conductivity. We therefore investigate whether incorporating the nanowires into the cosolvent or mixed cosolvent before addition to the PEDOT:PSS solution could lead to a better outcome. Here, we demonstrate that blending AgNWs into the cosolvent or mixed cosolvent before addition to PEDOT:PSS provides a better yet still simple method for embedding AgNWs into PEDOT:PSS to greatly enhance the conductivity of the hybrid films. The hybrid PEDOT:PSS films modified by mixed cosolvent that is preblended with AgNWs are found (on glass substrates) to show high visible-light transparency and a sheet resistance, R_s, of 104 Ω/□, which is among the lowest reported R_s values for as-deposited PEDOT:PSS films. These AgNW-embedded mixed-cosolvent-modified PEDOT:PSS films also exhibit a significant conductivity enhancement of 33% relative to that obtained with just mixed-cosolvent-modified PEDOT:PSS. Furthermore, we also obtain one of the highest ever reported efficiencies, greater than 15%, for HSCs fabricated with the highly conducting hybrid AgNW-embedded mixed-cosolvent-modified PEDOT:PSS films on planar n-type Si substrates, without the need for any complex surface texturing of the Si substrate, elaborate interface engineering, or expensive antireflective coating. Our results suggest that the formation of conducting PEDOT grains along the efficiently embedded AgNWs not only reduces the sheet resistance but also improves the antireflective properties, which together greatly increase the performance of HSCs.

RESULTS AND DISCUSSION

Two different solutions are used to embed AgNWs in PEDOT:PSS, and they are shown schematically in Figure 1a. A typical transmission electron microscopy (TEM) image of AgNWs used for the embedment is shown in Figure 1b, and a corresponding high-resolution TEM image shown in the inset depicts a lattice spacing of 0.236 nm corresponding to the (111) interplanar separation of the Ag face-centered cubic lattice.[33] The PEDOT:PSS solution mixed with an optimized 16 wt % of the mixed cosolvent from a stock 50:50 wt % mixture of EG and methanol (MeOH), which is designated here as EM16,[8] is also prepared for comparison. Solution AgNW-EM16 is obtained by preblending optimized 0.25 wt % AgNWs (suspended in isopropyl alcohol, IPA) in the mixed cosolvent solution first before adding the resulting AgNW-embedded mixed cosolvent solution to PEDOT:PSS, whereas a solution of AgNW+EM16 is obtained by adding AgNWs (suspended in IPA) to PEDOT:PSS premodified with the mixed cosolvent (*i.e.*, EM16). Appropriate aliquots of these solutions are then spin-coated (at an optimized spin rate of 4000 rpm, Figure S1) individually onto glass substrates. It should be noted that the fabrication of a AgNW film with AgNW-dispersed solution using spin-coating was not possible as it was not adhering to the glass substrate to form a uniform film. For comparison, the AgNW-suspended solution (0.25 wt % of stock solution diluted in IPA) is drop-casted on a glass substrate, which shows a sheet resistance of ∼26 Ω/□. The sheet resistances and conductivities of the EM16, AgNW-EM16, and AgNW+EM16 films are compared in Figure 1c, and their respective current−voltage (I−V) characteristics are shown in Figure 1d, with the schematic of the device structure depicted in Figure 1d, inset. The trend found for the I−V curves among the three films are in good accord with that for their corresponding sheet resistance results. The EM16 film (*i.e.*, without the AgNWs) shows a sheet resistance (R_s) of 138 Ω/□ (and conductivity of 906 S/cm). The AgNW-EM16 film, obtained by preblending an optimized 0.25 wt % AgNW solution with the mixed cosolvent before addition to

DOI: 10.1021/acsnano.8b04848
ACS Nano 2018, 12, 9495−9503

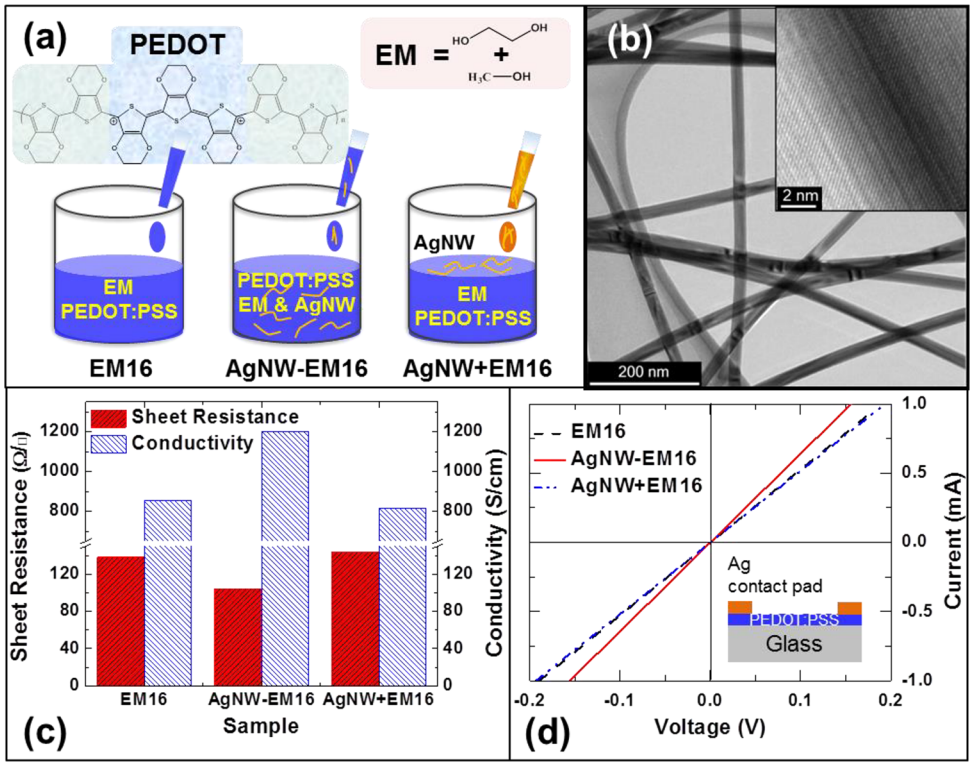

Figure 1. (a) Schematic diagram of solution preparation by mixed cosolvent addition in PEDOT:PSS (EM16), addition of the mixed cosolvent EM16 preblended with AgNWs in PEDOT:PSS (AgNW-EM16), and addition of AgNWs to EM16 (AgNW+EM16). Chemical structures of PEDOT with quinoid and benozid components and the mixture of cosolvents ethylene glycol (E) and methanol (M) are also shown. (b) Typical TEM and HRTEM images (inset) of AgNWs used for the embedment in PEDOT:PSS. (c) Sheet resistance and conductivity and (d) current−voltage (I−V) characteristics of EM16, AgNW-EM16, and AgNW+EM16 films deposited on glass substrates. Inset in (d) shows the schematic diagram of the device structure used for I−V characterization.

PEDOT:PSS, is found to show a ∼23% reduction in R_s to 104 Ω/□ (and an increase in its conductivity to 1202 S/cm). Employing a higher or lower amount of AgNWs from the optimized value in the mixed cosolvent (before adding to PEDOT:PSS) increases the R_s value and concomitantly reduces the conductivity (Figure S2) in comparison to that of the AgNW-EM16 film. On the other hand, the addition of 0.25 wt % AgNWs to mixed-cosolvent-modified PEDOT:PSS (AgNW+EM16) causes an increase in R_s to 141 Ω/□ (with a decrease in its conductivity to 887 S/cm), which is slightly higher than that of the EM16 film (Figure 1c). Similar results are also obtained for PEDOT:PSS films upon addition of cosolvent EG preblended with 0.25 wt % AgNWs (AgNW-E7, Figure S3), where R_s decreases (conductivity increases) from 170 Ω/□ (588 S/cm) for 7 wt % EG added PEDOT:PSS (denoted as E7)[8] to 132 Ω/□ (887 S/cm) for AgNW-E7. Evidently, the embedment of AgNWs in PEDOT:PSS by preblending the NWs in a mixed cosolvent prior to the addition to PEDOT:PSS (AgNW-EM16) has produced a performance superior to that of preblending the NWs in a single cosolvent EG (AgNW-E7). Preblending an optimized amount of 0.25 wt % AgNWs in the mixed cosolvent and then adding the AgNW-embedded mixed cosolvent to PEDOT:PSS can therefore produce a hybrid AgNW-PEDOT:PSS film with the lowest sheet resistance and the highest conductivity. The R_s value of 104 Ω/□ obtained for the AgNW-EM16 film is a significant result as this is among the lowest sheet resistance value ever reported for as-deposited PEDOT:PSS films.

To investigate the influence of the solvent (IPA) used to disperse the AgNWs on the conductivity enhancement of the PEDOT:PSS films, we prepare, in a separate experiment, PEDOT:PSS solutions with the same cosolvents as AgNW-EM16 and AgNW+EM16, that is, adding an aliquot of IPA but without any AgNWs. The deposited films show conductivities less than 800 S/cm irrespective of the IPA addition to the mixed cosolvent EM16 before or after PEDOT:PSS is premodified. It indicates that whereas the embedment of AgNWs in PEDOT:PSS could increase the conductivity, the enhancement is not caused by the solvent used to disperse the AgNWs. It also suggests that the conductivity of PEDOT:PSS could be further enhanced by employing an alternate solvent to disperse AgNWs to accommodate a higher concentration of AgNWs.

Scanning electron microscopy (SEM) and TEM can be used to determine the surface morphology and microstructures of AgNWs and PEDOT:PSS. Figure 2a,b shows the SEM images of AgNW-EM16 and AgNW+EM16 films, respectively. Schematic representations of AgNWs in PEDOT:PSS films on the Si/SiO_2 substrates are shown in the insets of Figure 2a,b, depicting the effects of the two embedment methods of AgNWs in PEDOT:PSS. Long intact AgNWs embedded in the PEDOT:PSS films are evident for the AgNW-EM16 sample (Figure 2a), whereas degradation of the long AgNWs are observed for the AgNW+EM16 (Figure 2b). Such a difference is also observed in the corresponding TEM images of these films (Figure 2c,d), where the (black) nanowire structure of the AgNWs obtained from AgNW-EM16 (PEDOT:PSS modified with a mixed cosolvent that is preblended with AgNWs) remains intact. However, breaking of the nanowires is found for the AgNWs added to mixed-cosolvent-modified

DOI: 10.1021/acsnano.8b04848
ACS Nano 2018, 12, 9495−9503

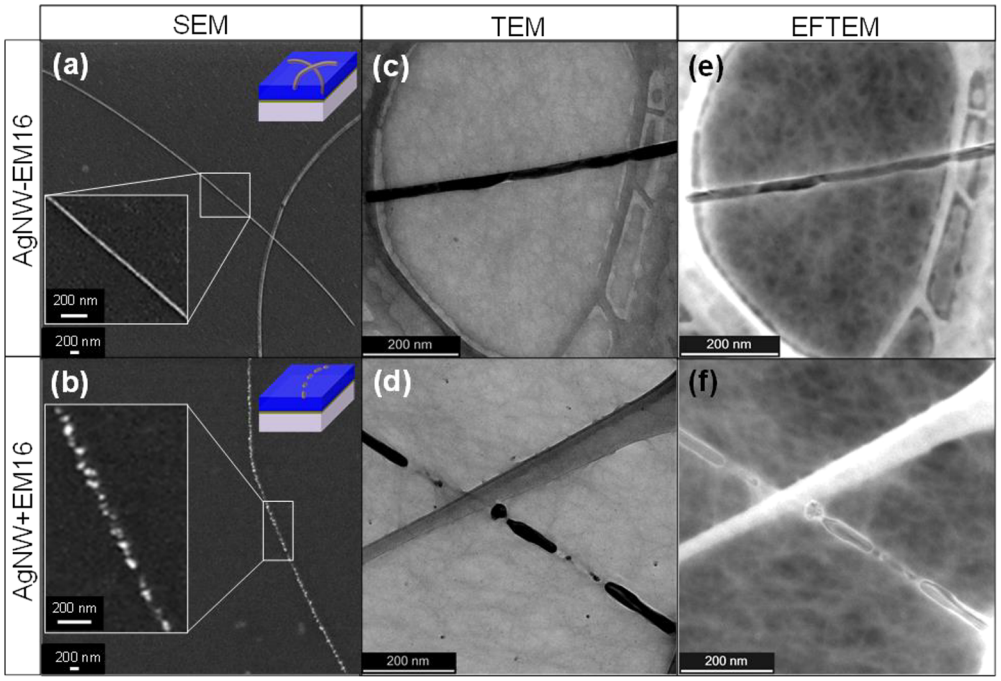

Figure 2. (a,b) SEM, (c,d) TEM, and (e,f) EFTEM of AgNW-EM16 (a,c,e) and AgNW+EM16 (b,d,f) samples. The left insets in (a,b) show magnified views of the marked areas. The top-right insets in (a,b) show 3D schematic representations of AgNWs embedded in PEDOT:PSS on Si/SiO_2 substrates. The TEM and EFTEM images are collected for the films deposited on TEM grids.

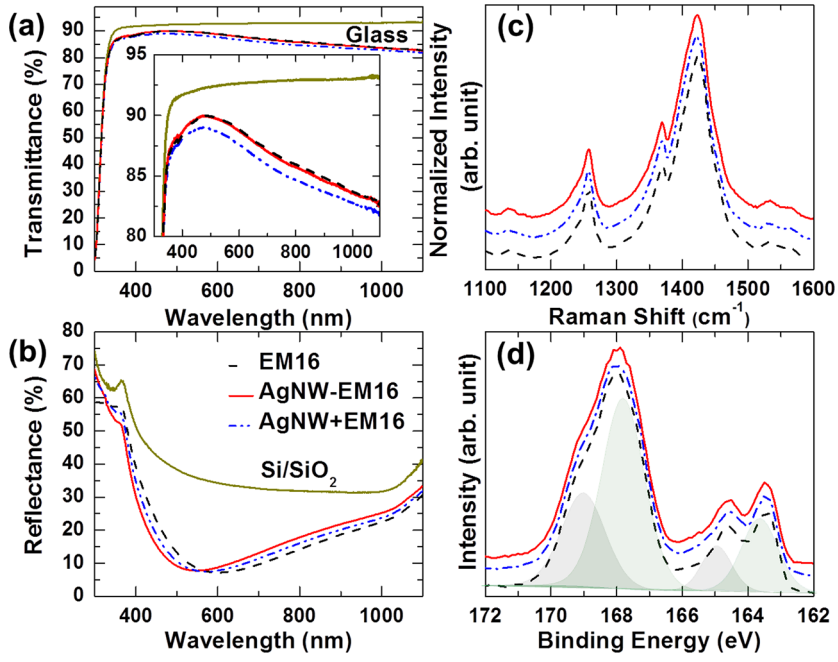

Figure 3. (a) Transmittance, (b) reflectance, (c) Raman, and (d) XPS S 2p spectra of EM16, AgNW-EM16, and AgNW+EM16 films on glass substrates (a) and on Si/SiO_2 substrates (b–d). For comparison, the transmittance spectrum of a glass substrate and reflectance spectrum of a Si/SiO_2 substrate are included in (a,b), respectively. The inset in (a) shows a magnified view of the transmittance spectra.

PEDOT:PSS (AgNW+EM16). Earlier, we reported the use of a low-energy-loss (plasmon) energy-filtered TEM (EFTEM) imaging technique to observe the PEDOT:PSS grains of cosolvent-modified PEDOT:PSS.[8] The low-energy-loss EFTEM study can be used to accentuate the bright insulating PSS chains from the darker highly conducting PEDOT grains in the TEM images. Furthermore, the peripheries of the long AgNWs generally appear less bright (Figure 2e) than the brighter deteriorated/broken segments of AgNWs (Figure 2f), which indicates that the insulating PSS moieties surround the broken AgNW segments more extensively than the properly embedded uninterrupted AgNWs in PEDOT:PSS.

The transmittance spectra of all the PEDOT:PSS films on glass substrates in Figure 3a show very high transmittance with a maximum at 480 nm greater than 89% but slightly less than that of the bare glass substrate. A slightly higher transmittance in the 380–1100 nm region is found for the EM16 and AgNW-EM16 samples compared to that of the AgNW+EM16

DOI: 10.1021/acsnano.8b04848
ACS Nano 2018, 12, 9495–9503

sample (Figure 3a, inset). Remarkably, effective embedment of AgNWs in PEDOT:PSS in the AgNW-EM16 sample has preserved its high transparency, similar to the EM16 film. The estimated figure of merit values of EM16, AgNW-EM16, and AgNW+EM16 films are 0.65, 0.86, and 0.63, respectively. The highly transparent and conducting nature of these films reinforces its potential for use in transparent conductive electronic devices. As the antireflective property of PEDOT:PSS films on Si/SiO_2 substrates is a well-known advantage for improving the photovoltaic properties, we compare, in Figure 3b, the reflectance spectra of the films, before and after the embedment of AgNWs in PEDOT:PSS, on Si/SiO_2 substrates along with that of a typical (bare) Si/SiO_2 substrate. All the PEDOT:PSS films show similarly high antireflective properties with reflectance minima less than 8.0% near 550 nm. Interestingly, the reflectance minimum of the AgNW-EM16 sample at 548 nm exhibits small blue shifts of ~27 and ~51 nm relative to the AgNW+EM16 and EM16 samples, respectively.

Our results show that the AgNW-EM16 film exhibits a lower sheet resistance and a higher conductivity than the EM16 and AgNW+EM16 films (Figure 1c). The AgNW-EM16 film also shows a transmittance spectrum slightly lower than that of the EM16 film (Figure 3a), in contrast to the discernibly lower transmittance found for the AgNW+EM16 film as a result of the degradation of AgNWs. All the films appear to show similar reflectance minima %, with the highest antireflective property (lowest reflectance) near the blue wavelength range (400−580 nm) observed for the AgNW-EM16 film. This antireflective property is likely due to the presence of AgNWs and its surrounding medium, in addition to the plasmonic and scattering effects of the NWs. Even though the addition of AgNWs to the mixed-cosolvent-premodified PEDOT:PSS (AgNW+NW16) results in the deterioration of NWs into broken NW segments and nanoparticles (Figure 2b), the AgNW+EM16 film shows an antireflective property near the blue wavelength range (with a blue shift in the reflectance minimum to a slightly lower wavelength) slightly better than that of the EM16 film because of the scattering effects of broken NWs.[34] The high antireflective properties of AgNW-embedded PEDOT:PSS film are found to be advantageous in enhancing the HSC properties, as discussed below.

Figure 3c,d shows the respective Raman spectra and XPS S 2p spectra of AgNW-EM16, AgNW+EM16, and EM16 films on Si/SiO_2 substrates. No significant differences are observed from these spectra. In accord with the typical Raman features of PEDOT reported in the literature,[35−37] the observed Raman features correspond to the symmetric stretching modes of quinoid ($C_\alpha-C_\beta$ at 1425 cm^{-1}) and benzoid ($C_\alpha=C_\beta$ at 1453 cm^{-1}), the asymmetric stretching modes of $C_\alpha-C_\beta$ (at 1530 and 1568 cm^{-1}), and the stretching vibrations of $C_\beta=C_\beta$ (at 1366 cm^{-1}) and $C_\alpha=C_{\alpha'}$ (between 1200 and 1300 cm^{-1}). The XPS spectra show two S 2p bands, each corresponding to a doublet of S $2p_{3/2}$ and S $2p_{1/2}$ components with a 1.2 eV spin−orbit splitting and a 2:1 intensity ratio. The weaker S $2p_{3/2}$ ($2p_{1/2}$) peak at 163.7 eV (164.9 eV) corresponds to the sulfur atoms of PEDOT, whereas the stronger S $2p_{3/2}$ ($2p_{1/2}$) peak at 167.8 eV (169.0 eV) corresponds to PSS. Insignificant variations in the intensity ratios of the PEDOT to PSS features indicate that the top surface structure modified by the mixed cosolvent in PEDOT:PSS is mostly preserved irrespective of the embedment methods of AgNWs to PEDOT:PSS.[6,7]

A HSC fabricated with the highly conducting hybrid AgNW-EM16 film deposited on a planar n-type Si/SiO_2 substrate is also found to exhibit exceptional photovoltaic performance. Figure 4 shows the current density *versus* voltage ($J-V$) curves

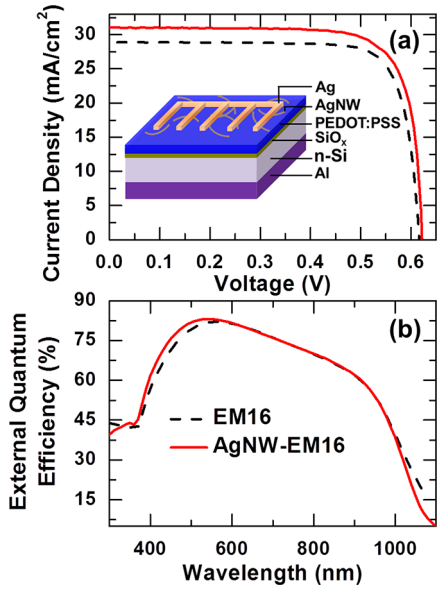

Figure 4. Photovoltaic properties of HSCs made from AgNW-EM16 and EM16 films deposited on planar Si/SiO_2 substrates. (a) Current density *vs* voltage and (b) external quantum efficiency curves of the AgNW-EM16-based and EM16-based HSCs. The inset in (a) shows a schematic diagram of the device structure of the AgNW-EM16-based HSC.

and external quantum efficiency (EQE) spectra of the fabricated HSCs, along with the device structure shown schematically as an inset. The highest power conversion efficiency (PCE) of 15.1%, along with V_{OC} of 622 mV, J_{SC} of 31.05 mA/cm^2, and FF of 78%, is obtained for the best-performance AgNW-EM16 cell. Reproducibly high PCE values have also been achieved for the other HSCs in the set of similarly prepared AgNW-EM16 HSCs (Table S1). For comparison, we also prepare an EM16-based HSC (*i.e.*, without the embedment of AgNWs), which shows a lower PCE of 14.3%, along with V_{OC} of 617 mV, J_{SC} of 28.85 mA/cm^2, and FF of 80%. The AgNW-EM16 cell shows slightly lower series (1.4 Ω cm^2) and shunt resistances (644 Ω cm^2) in comparison to that of the EM16 cell (1.8 and 987 Ω cm^2, respectively). The slightly higher FF (by 2%), likely arising from its higher shunt resistance, is observed for the best EM16 cell when compared to the highest-efficiency AgNW-EM16 cell. The higher shunt resistance is likely the result of the smooth surface characteristics[8] that enable better contact with the Ag top grid and thus more efficient carrier collection. The cells made from AgNW-EM16 exhibit PCEs nearly a full percent (0.8%) higher than that of the EM16 cell. In addition, the solar cells measured in the dark show typical diode characteristics. The EQE spectrum for the AgNW-EM16 cell also shows a discernibly higher efficiency in the lower wavelength (blue) region (compared to that of the EM16 cell), which is in good accord with the observed enhancement in the antireflective property (Figure 3b). It is clear that the structural modification obtained for the PEDOT:PSS films modified with mixed cosolvent preblended with AgNWs results in lower sheet resistance and higher antireflectance that lead to

DOI: 10.1021/acsnano.8b04848
ACS Nano 2018, 12, 9495−9503

the improvement in the front carrier collection and the overall solar cell performance.

The consequence of different methods of embedding AgNWs into cosolvent-modified PEDOT:PSS that trigger structural modifications of AgNWs and PEDOT:PSS is schematically illustrated in Figure 5. The 3D chemical

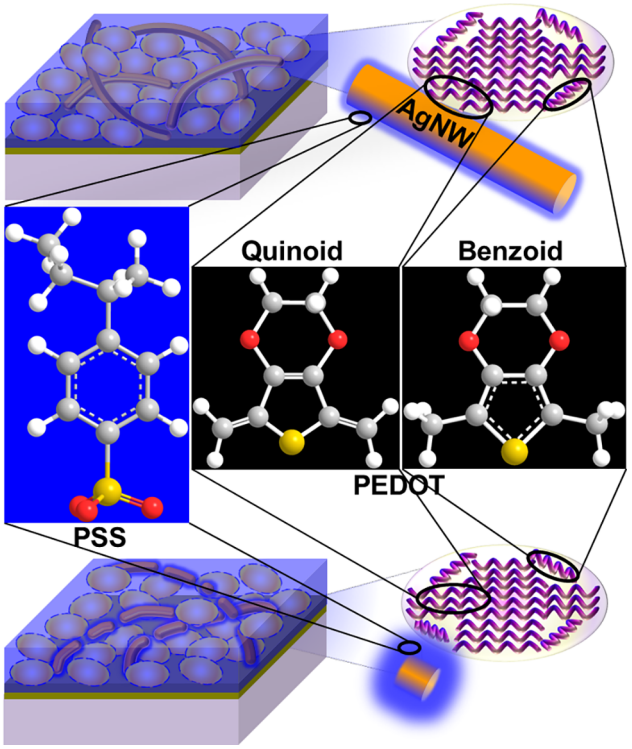

Figure 5. Schematic representations of AgNWs embedded in PEDOT:PSS with mixed cosolvent preblended with nanowires prior to addition into PEDOT:PSS (top) and AgNWs added to the mixed-cosolvent-modified PEDOT:PSS (bottom). The 3D chemical structures of PSS (center-left), quinoid (center-middle), and benzoid (center-right) chains present in the PEDOT:PSS matrix are shown along with its possible chain formation mechanism affected by the AgNW embedment process.

structures of the highly conducting quinoid and less conducting benzoid components of PEDOT and of the insulating PSS chains are also shown in the figure (center). It is well-known that the addition of a cosolvent would lead to the formation of ellipsoidal PEDOT grains surrounded by PSS.[5,38] Moreover, a mixture of appropriate cosolvents (mixed cosolvent) in the PEDOT:PSS further enhances not just the formation of PEDOT grains but also the coverage of a thinner layer of PSS, with the excess PSS in the matrix possibly either segregated to the voids between the grain boundaries or spun away during the spin-coating step.[8] As the separation of PSS from PEDOT by MeOH is well-known,[13,39] the mixed cosolvent (containing both EG and MeOH) could also facilitate such PSS separation. The separated PSS could be removed during the spin-coating process[39] and/or subsequently connected back to PEDOT *via* an EG interface,[40] which is schematically shown in Figure S4. The reduction of the coil-like benzoid structures that are located along the grain boundaries to a more linear or extended quinoid structure is also enhanced by the mixed cosolvent.[8,36,41] The addition of AgNWs in the mixed cosolvent promotes the formation of aligned PEDOT grains along the nanowires while preserving the lengths and structures of the nanowires. The close packing of PEDOT grains induced by the mixed cosolvent is preserved when AgNWs are incorporated into the cosolvent prior to addition into the PEDOT:PSS solution, and this close packing evidently aids in maintaining the high transmittance properties of the films. Furthermore, it is possible that the highly conducting quinoid chains (on the perimeters of the PEDOT grains) are in physical contact with the AgNWs that are connecting to the neighboring PEDOT grains. The AgNWs therefore serve as conduits that facilitate the charge-transfer process and improve the conductivity.

The presence of brighter regions around the broken AgNW segments in the EFTEM image (Figure 2f) suggests that these broken segments are covered by segregated insulating PSS moieties. It is possible that when subjecting the AgNWs to the mixed-cosolvent-premodified PEDOT:PSS, where the PEDOT grain formation has already occurred (before the arrival of the NWs), the excess PSS moieties in the PEDOT grain boundaries tend to engulf the AgNWs, initiating the etching of AgNWs due to the acidic nature of the PSS. Further etching is accelerated at these initially etched active sites, causing the breaking of nanowires and, subsequently, the observed increase in the sheet resistance. Moreover, the quinoid chains remain inside the PEDOT grains, and the grain boundaries are populated with the benzoid chains. As the broken AgNWs are surrounded by the PSS moieties, the peripheries of PEDOT grains interacting with the broken AgNWs are also likely filled with benzoid chains. This results in less charge transfer, causing lower conductivity. Proper embedment of AgNWs in PEDOT:PSS therefore facilitates the interaction of the extended quinoid chains and charge transfer with the nanowires, increasing the conductivity. Indeed, the sheet resistance of the AgNW-EM16 film (104 Ω/□) is comparable to that of the commercially available ITO-coated polyethylene terephthalate (~60 to 300 Ω/□) or ITO-coated glass (~8 to 100 Ω/□) substrates, which illustrates the potential of its commercial application in low-cost transparent conductive and flexible electronic devices. The lower sheet resistance and higher antireflective properties of the AgNW-EM16 film are the main contributors to the higher efficiencies in these HSCs. The HSC fabricated with the efficiently embedded AgNW-EM16 film exhibits the highest PCE of 15.1%, which is among the highest efficiency ever reported for a planar HSC to date without the need for any additional antireflective coating or interlayers.

CONCLUSION

In summary, we present a simple method of effectively embedding AgNWs in a PEDOT:PSS solution to improve the conductivity and efficiency of a HSC. Mixing AgNWs to a cosolvent or mixed cosolvent prior to addition into PEDOT:PSS (AgNW-EM16) is important to preserving the integrity of the nanowires while engineering the PEDOT:PSS structure. This approach enables us to achieve a AgNW-embedded mixed-cosolvent-modified PEDOT:PSS film with a significantly higher conductivity of 1202 S/cm in comparison to that of the EM16 film (906 S/cm) and a high overall visible-light transparency greater than 85%. Our data suggest that the highly conducting form of quinoid chains in the PEDOT grains is in contact with the long AgNWs that are interconnecting the nearby grains. The AgNWs work as channels for promoting the charge-transfer process and thereby improve the conductivity.

DOI: 10.1021/acsnano.8b04848
ACS Nano 2018, 12, 9495−9503

On the other hand, the addition of AgNWs after the mixed cosolvent modification of PEDOT:PSS (AgNW+EM16) causes deterioration of the nanowires and contributes to the increase in the sheet resistance in comparison to mixed-cosolvent-modified PEDOT:PSS (EM16). The hybrid solar cell made from a AgNW-EM16 film on a planar silicon substrate shows a very high V_{OC} of 622 mV and a record high PCE of 15.1%. Indeed, the PCE achieved in this work is among the highest efficiency ever reported for planar single-junction HSCs, without the use of any antireflective or back material coating and complex fabrication of silicon nanostructures. These and other additional processing including post-treatment of the AgNW-EM16 film, solar cell fabrication on surface-structured silicon substrates, interface engineering, and antireflective coating on PEDOT:PSS film are expected to further enhance the HSC performance. The present simple approach of efficiently embedding nanowires in PEDOT:PSS can also be extended to incorporate other similar nanowires and nanoparticles by fine-tuning their dimensions and their concentrations in the dispersion and by choosing a suitable dispersing solvent, which could be beneficial to advancing the performances of the organic−organic or organic−inorganic electronic devices.

EXPERIMENTAL DETAILS

Preparation of AgNW-Embedded PEDOT:PSS Solutions. Highly conducting-grade PEDOT:PSS (PH1000), AgNWs (AgNW-25, 1 wt % suspension in IPA) with an average diameter of 15−35 nm and an average length of 15−30 μm, and all other chemicals were purchased from commercial sources and used as-received unless otherwise specified. The PEDOT:PSS solution was filtered through a 0.45 μm PVDF syringe filter prior to being mixed with the solvents or AgNWs. Initially, a stock cosolvent mixture of 50 wt % EG and 50 wt % MeOH was prepared. Typical solution preparation processes are schematically shown in Figure 1a. The PEDOT:PSS solution was added to an optimized 16 wt % solution of the stock mixture of mixed cosolvent (denoted as EM16) mixed with IPA solutions of different wt % (0.1, 0.25, 0.5, and 0.75) suspensions of AgNWs. After the sheet resistance studies, the PEDOT:PSS solution added with mixed cosolvent EM16 preblended with an optimized 0.25 wt % AgNWs solution was found to exhibit the lowest sheet resistance (Figure S1). This film was used for further device fabrication and characterization. The film samples prepared using such a solution containing 0.25 wt % AgNWs are designated here as AgNW-EM16 (Figure 1a). For comparison, 16 wt % of mixed-cosolvent-modified PEDOT:PSS solution (EM16) and EM16 subsequently blended with 0.25 wt % AgNWs (designated as AgNW+EM16, Figure 1a) were separately prepared. Other sets of solutions were also prepared by using 0.25 and 0.5 wt % AgNWs premixed with an appropriately optimized amount of 7 wt % EG. The resulting solution preblended with an optimized 0.25 wt % AgNW solution was then added to PEDOT:PSS (AgNW-E7). A PEDOT:PSS solution just added with 7 wt % EG without employing any AgNWs (E7) was also prepared. Prior to spin-coating an appropriate amount of the modified PEDOT:PSS solutions onto the substrates, 0.25 wt % fluorosurfactant (FS-300) was also added to improve the wettability of the solutions on glass and Si/SiO_2 substrates.

Hybrid AgNW-PEDOT:PSS Film Preparation and HSC Fabrication. The films deposited on glass substrates were used for sheet resistance and transmittance property studies. Phosphorus-doped, n-type Si(100) substrates (380 ± 25 μm thick, Virginia Semiconductor Inc.), with a resistivity of 0.05−0.10 Ω·cm, were used for solar cell device fabrication and for other characterizations. Details of the PEDOT:PSS film preparation and device fabrication processes have been reported elsewhere.[8,11] Briefly, an appropriate aliquot of the PEDOT:PSS solution modified with a cosolvent or a mixed cosolvent with or without preblending with AgNWs was spin-coated on appropriately cleaned glass substrates and then subsequently annealed at 109 ± 1 °C on a hot plate in air for 10 min. Initially, the films were deposited on glass substrates at four different spin rates of 2000, 4000, 6000, and 8000 rpm. An optimized spin rate of 4000 rpm was found to give the lowest measured sheet resistance values and was therefore chosen for all subsequent depositions (Figure S1). Cleaned Si substrates were immersed in 5% hydrofluoric acid for 2 min to remove the native oxide layer, followed by thorough rinsing in filtered high-resistivity (18.2 MΩ) water. An aluminum metal bottom electrode (200 nm thick) was then deposited on the unpolished side of the Si substrate in a dual-target magnetron sputtering system (EMS575X). As it was important to form an appropriately optimized interface oxide layer prior to the PEDOT:PSS deposition on the Si substrates,[11] the Si substrates were kept in ambient atmosphere for at least 20−60 min to form a SiO_x layer after the bottom electrode deposition. We denoted the resulting substrates as Si/SiO_2 substrates. A shadow mask was used to deposit the top comb-type silver metal grid electrode (50 nm thick) on the polymer layer for HSC characterization.

Characterization of PEDOT:PSS Films and HSCs. The sheet resistances and current−voltage characteristics were measured by using the four-point probe method in a van der Pauw configuration (Ecopia HMS-5300). The transmittance and reflectance spectra of the films were obtained in a UV−vis spectrophotometer (PerkinElmer Lambda 35). The Raman spectra were collected at room temperature with a laser wavelength of 785 nm and laser power of 10 mW in a Bruker Senterra Raman confocal microscope. X-ray photoelectron spectroscopy studies were carried out in a Thermo-VG Scientific ESCALab 250 microprobe. The spectra were obtained using a monochromatic Al Kα source (1486.6 eV), and CasaXPS software was used for peak fitting (after correction with the Shirley background). The surface morphologies of the films were examined by scanning electron microscopy in a Zeiss LEO 1530 microscope. Transmission electron microscopy measurements were carried out in a Zeiss Libra 200 MC microscope operated at 200 keV. Low-energy-loss (or plasmon) energy-filtered TEM images were acquired by using an exit slit with an appropriate slit width for the double-corrected omega energy filter.[8]

The solar cell measurement methods have been reported previously.[11] Briefly, the solar cell properties were analyzed by using a solar cell characterization system capable of both $I-V$ and EQE measurements (PV Measurements IV5 and QEX10). The $I-V$ measurements were performed under 100 mW/cm^2 (1 Sun) illumination using a class ABA solar simulator (with an AM 1.5G filter) in air. Prior to the $I-V$ measurement, a Si reference cell (PVM782 with a BK7 window) was used to calibrate the light source intensity. An aluminum metal aperture mask was used to define the area of the device (7 × 7 mm^2) during the $I-V$ measurement. The EQE measurements were carried out under monochromatic light (in between two fingers of the top comb electrode), as filtered by a dual-grating monochromator from a xenon arc lamp source, coupled with a germanium photodiode. The approximate illumination area for the EQE measurements was 1 × 3.5 mm^2.

ASSOCIATED CONTENT

Supporting Information

The Supporting Information is available free of charge on the ACS Publications website at DOI: 10.1021/acsnano.8b04848.

Supplemental sheet resistance and conductivity data, schematic 2D structure representations of PEDOT:PSS with and without an EG interface, and photovoltaic properties of five different AgNW-EM16 cells (PDF)

AUTHOR INFORMATION

Corresponding Author

*E-mail: tong@uwaterloo.ca.

ORCID

Joseph P. Thomas: 0000-0001-6455-908X

DOI: 10.1021/acsnano.8b04848
ACS Nano 2018, 12, 9495−9503

Kam Tong Leung: 0000-0002-1879-2806

Notes

The authors declare no competing financial interest.

ACKNOWLEDGMENTS

This work was supported by the Natural Sciences and Engineering Research Council of Canada.

REFERENCES

(1) Liu, R.; Wang, J.; Sun, T.; Wang, M.; Wu, C.; Zou, H.; Song, T.; Zhang, X.; Lee, S.-T.; Wang, Z. L.; Sun, B. Silicon Nanowire/Polymer Hybrid Solar Cell-Supercapacitor: A Self-Charging Power Unit with a Total Efficiency of 10.5%. *Nano Lett.* **2017**, *17*, 4240−4247.

(2) Ouyang, J.; Chu, C.-W.; Chen, F.-C.; Xu, Q.; Yang, Y. High-Conductivity Poly(3,4-ethylenedioxythiophene):Poly-(styrenesulfonate) Film and Its Application in Polymer Optoelectronic Devices. *Adv. Funct. Mater.* **2005**, *15*, 203−208.

(3) Bubnova, O.; Khan, Z. U.; Wang, H.; Braun, S.; Evans, D. R.; Fabretto, M.; Hojati-Talemi, P.; Dagnelund, D.; Arlin, J. B.; Geerts, Y. H.; Desbief, S.; Breiby, D. W.; Andreasen, J. W.; Lazzaroni, R.; Chen, W. M.; Zozoulenko, I.; Fahlman, M.; Murphy, P. J.; Berggren, M.; Crispin, X. Semi-Metallic Polymers. *Nat. Mater.* **2014**, *13*, 190−194.

(4) Liu, Z.; Yang, Z.; Wu, S.; Zhu, J.; Guo, W.; Sheng, J.; Ye, J.; Cui, Y. Photoinduced Field-Effect Passivation from Negative Carrier Accumulation for High-Efficiency Silicon/Organic Heterojunction Solar Cells. *ACS Nano* **2017**, *11*, 12687−12695.

(5) Kim, N.; Kee, S.; Lee, S. H.; Lee, B. H.; Kahng, Y. H.; Jo, Y.-R.; Kim, B.-J.; Lee, K. Highly Conductive PEDOT:PSS Nanofibrils Induced by Solution-Processed Crystallization. *Adv. Mater.* **2014**, *26*, 2268−2272.

(6) Thomas, J. P.; Zhao, L.; McGillivray, D.; Leung, K. T. High-Efficiency Hybrid Solar Cells by Nanostructural Modification in PEDOT:PSS with Co-Solvent Addition. *J. Mater. Chem. A* **2014**, *2*, 2383−2389.

(7) Crispin, X.; Jakobsson, F. L. E.; Crispin, A.; Grim, P. C. M.; Andersson, P.; Volodin, A.; van Haesendonck, C.; Van der Auweraer, M.; Salaneck, W. R.; Berggren, M. The Origin of the High Conductivity of Poly(3,4-ethylenedioxythiophene)-Poly-(styrenesulfonate) (PEDOT-PSS) Plastic Electrodes. *Chem. Mater.* **2006**, *18*, 4354−4360.

(8) Thomas, J. P.; Leung, K. T. Mixed Co-Solvent Engineering of PEDOT:PSS to Enhance Its Conductivity and Hybrid Solar Cell Properties. *J. Mater. Chem. A* **2016**, *4*, 17537−17542.

(9) Zhang, W.; Zhao, B.; He, Z.; Zhao, X.; Wang, H.; Yang, S.; Wu, H.; Cao, Y. High-Efficiency ITO-Free Polymer Solar Cells Using Highly Conductive PEDOT:PSS/surfactant Bilayer Transparent Anodes. *Energy Environ. Sci.* **2013**, *6*, 1956−1964.

(10) Liu, Q.; Ono, M.; Tang, Z.; Ishikawa, R.; Ueno, K.; Shirai, H. Highly Efficient Crystalline Silicon/Zonyl Fluorosurfactant-Treated Organic Heterojunction Solar Cells. *Appl. Phys. Lett.* **2012**, *100*, 183901.

(11) Thomas, J. P.; Leung, K. T. Defect-Minimized PEDOT:PSS/Planar-Si Solar Cell with Very High Efficiency. *Adv. Funct. Mater.* **2014**, *24*, 4978−4985.

(12) Kim, Y. H.; Sachse, C.; Machala, M. L.; May, C.; Müller-Meskamp, L.; Leo, K. Highly Conductive PEDOT:PSS Electrode with Optimized Solvent and Thermal Post-Treatment for ITO-Free Organic Solar Cells. *Adv. Funct. Mater.* **2011**, *21*, 1076−1081.

(13) McGillivray, D.; Thomas, J. P.; Abd-Ellah, M.; Heinig, N. F.; Leung, K. T. Performance Enhancement by Secondary Doping in PEDOT:PSS/Planar-Si Hybrid Solar Cells. *ACS Appl. Mater. Interfaces* **2016**, *8*, 34303−34308.

(14) Li, Q.; Yang, J.; Chen, S.; Zou, J.; Xie, W.; Zeng, X. Highly Conductive PEDOT:PSS Transparent Hole Transporting Layer with Solvent Treatment for High Performance Silicon/Organic Hybrid Solar Cells. *Nanoscale Res. Lett.* **2017**, *12*, 506.

(15) Kim, N.; Kang, H.; Lee, J. H.; Kee, S.; Lee, S. H.; Lee, K. Highly Conductive All-Plastic Electrodes Fabricated Using a Novel Chemically Controlled Transfer-Printing Method. *Adv. Mater.* **2015**, *27*, 2317−2323.

(16) Ouyang, J. Secondary Doping" Methods to Significantly Enhance the Conductivity of PEDOT:PSS for Its Application as Transparent Electrode of Optoelectronic Devices. *Displays* **2013**, *34*, 423−436.

(17) Thomas, J. P.; Srivastava, S.; Zhao, L.; Abd-Ellah, M.; McGillivray, D.; Kang, J. S.; Rahman, M. A.; Moghimi, N.; Heinig, N. F.; Leung, K. T. Reversible Structural Transformation and Enhanced Performance of PEDOT:PSS-Based Hybrid Solar Cells Driven by Light Intensity. *ACS Appl. Mater. Interfaces* **2015**, *7*, 7466−7470.

(18) Louarn, G.; Trznadel, M.; Buisson, J. P.; Laska, J.; Pron, A.; Lapkowski, M.; Lefrant, S. Raman Spectroscopic Studies of Regioregular Poly (3-Alkylthiophenes). *J. Phys. Chem.* **1996**, *100*, 12532−12539.

(19) Garreau, S.; Louarn, G.; Buisson, J. P.; Froyer, G.; Lefrant, S. In Situ Spectroelectrochemical Raman Studies of Poly(3,4-ethylenedioxythiophene) (PEDT). *Macromolecules* **1999**, *32*, 6807−6812.

(20) Kim, T.; Kim, Y. W.; Lee, H. S.; Kim, H.; Yang, W. S.; Suh, K. S. Uniformly Interconnected Silver-Nanowire Networks for Transparent Film Heaters. *Adv. Funct. Mater.* **2013**, *23*, 1250−1255.

(21) Chen, T.-G.; Huang, B.-Y.; Liu, H.-W.; Huang, Y.-Y.; Pan, H.-T.; Meng, H.-F.; Yu, P. Flexible Silver Nanowire Meshes for High-Efficiency Microtextured Organic-Silicon Hybrid Photovoltaics. *ACS Appl. Mater. Interfaces* **2012**, *4*, 6857−6864.

(22) Kim, S.; Kim, S. Y.; Kim, J.; Kim, J. H. Highly Reliable AgNW/PEDOT:PSS Hybrid Films: Efficient Methods for Enhancing Transparency and Lowering Resistance and Haziness. *J. Mater. Chem. C* **2014**, *2*, 5636−5643.

(23) Xu, Q.; Song, T.; Cui, W.; Liu, Y.; Xu, W.; Lee, S.-T.; Sun, B. Solution-Processed Highly Conductive PEDOT:PSS/AgNW/GO Transparent Film for Efficient Organic-Si Hybrid Solar Cells. *ACS Appl. Mater. Interfaces* **2015**, *7*, 3272−3279.

(24) Jiang, X.; Zhang, P.; Zhang, J.; Wang, J.; Li, G.; Fang, X.; Yang, L.; Chen, X. High Performance of PEDOT:PSS/n-Si Solar Cells Based on Textured Surface with AgNWs Electrodes. *Nanoscale Res. Lett.* **2018**, *13*, 53.

(25) Um, H.-D.; Choi, D.; Choi, A.; Seo, J. H.; Seo, K. Embedded Metal Electrode for Organic-Inorganic Hybrid Nanowire Solar Cells. *ACS Nano* **2017**, *11*, 6218−6224.

(26) Yang, Z.; Gao, P.; He, J.; Chen, W.; Yin, W.-Y.; Zeng, Y.; Guo, W.; Ye, J.; Cui, Y. Tuning of the Contact Properties for High-Efficiency Si/PEDOT:PSS Heterojunction Solar Cells. *ACS Energy Lett.* **2017**, *2*, 556−562.

(27) Han, Y.; Liu, Y.; Yuan, J.; Dong, H.; Li, Y.; Ma, W.; Lee, S.-T.; Sun, B. Naphthalene Diimide-Based n-Type Polymers: Efficient Rear Interlayers for High-Performance Silicon-Organic Heterojunction Solar Cells. *ACS Nano* **2017**, *11*, 7215−7222.

(28) Jeong, H.; Song, H.; Pak, Y.; Kwon, I. K.; Jo, K.; Lee, H.; Jung, G. Y. Enhanced Light Absorption of Silicon Nanotube Arrays for Organic/Inorganic Hybrid Solar Cells. *Adv. Mater.* **2014**, *26*, 3445−3450.

(29) Sharma, M.; Pudasaini, P. R.; Ruiz-Zepeda, F.; Elam, D.; Ayon, A. A. Ultrathin, Flexible Organic−Inorganic Hybrid Solar Cells Based on Silicon Nanowires and PEDOT:PSS. *ACS Appl. Mater. Interfaces* **2014**, *6*, 4356−4363.

(30) Wang, H.-P.; Lin, T.-Y.; Tsai, M.-L.; Tu, W.-C.; Huang, M.-Y.; Liu, C.-W.; Chueh, Y.-L.; He, J.-H. Toward Efficient and Omnidirectional n-Type Si Solar Cells: Concurrent Improvement in Optical and Electrical Characteristics by Employing Microscale Hierarchical Structures. *ACS Nano* **2014**, *8*, 2959−2969.

(31) Zielke, D.; Pazidis, A.; Werner, F.; Schmidt, J. Organic-Silicon Heterojunction Solar Cells on n-Type Silicon Wafers: The Back-PEDOT Concept. *Sol. Energy Mater. Sol. Cells* **2014**, *131*, 110−116.

(32) Liu, Q.; Ishikawa, R.; Funada, S.; Ohki, T.; Ueno, K.; Shirai, H. Highly Efficient Solution-Processed Poly(3,4-ethylenedioxythiophene):Poly(styrenesulfonate)/Crystalline-Silicon Heterojunc-

DOI: 10.1021/acsnano.8b04848
ACS Nano 2018, 12, 9495−9503

tion Solar Cells with Improved Light-Induced Stability. *Adv. Energy Mater.* **2015**, *5*, 1500744.
(33) Radmilović, V. V.; Göbelt, M.; Ophus, C.; Christiansen, S.; Spiecker, E.; Radmilović, V. R. Low Temperature Solid-State Wetting and Formation of Nanowelds in Silver Nanowires. *Nanotechnology* **2017**, *28*, 385701.
(34) Mock, J. J.; Barbic, M.; Smith, D. R.; Schultz, D. A.; Schultz, S. Shape Effects in Plasmon Resonance of Individual Colloidal Silver Nanoparticles. *J. Chem. Phys.* **2002**, *116*, 6755−6759.
(35) Schaarschmidt, A.; Farah, A. A.; Aby, A.; Helmy, A. S. Influence of Nonadiabatic Annealing on the Morphology and Molecular Structure of PEDOT-PSS Films. *J. Phys. Chem. B* **2009**, *113*, 9352−9355.
(36) Lapkowski, M.; Pron, A. Electrochemical Oxidation of Poly (3,4-Ethylenedioxythiophene)— "'in Situ'" Conductivity and Spectroscopic Investigations. *Synth. Met.* **2000**, *110*, 79−83.
(37) Chiu, W. W.; Travaš-Sejdić, J.; Cooney, R. P.; Bowmaker, G. A. Studies of Dopant Effects in Poly(3,4-ethylenedi-oxythiophene) Using Raman Spectroscopy. *J. Raman Spectrosc.* **2006**, *37*, 1354−1361.
(38) Ugur, A.; Katmis, F.; Li, M.; Wu, L.; Zhu, Y.; Varanasi, K. K.; Gleason, K. K. Low-Dimensional Conduction Mechanisms in Highly Conductive and Transparent Conjugated Polymers. *Adv. Mater.* **2015**, *27*, 4604−4610.
(39) Alemu, D.; Wei, H.-Y.; Ho, K.-C.; Chu, C.-W. Highly Conductive PEDOT:PSS Electrode by Simple Film Treatment with Methanol for ITO-Free Polymer Solar Cells. *Energy Environ. Sci.* **2012**, *5*, 9662−9671.
(40) Alemu Mengistie, D.; Wang, P.-C.; Chu, C.-W. Effect of Molecular Weight of Additives on the Conductivity of PEDOT:PSS and Efficiency for ITO-Free Organic Solar Cells. *J. Mater. Chem. A* **2013**, *1*, 9907−9915.
(41) Kim, N.; Kee, S.; Lee, S. H.; Lee, B. H.; Kahng, Y. H.; Jo, Y.-R.; Kim, B.-J.; Lee, K. Highly Conductive PEDOT : PSS Nanofibrils Induced by Solution-Processed Crystallization. *Adv. Mater.* **2014**, *26*, 2268−2272.

DOI: 10.1021/acsnano.8b04848
ACS Nano 2018, 12, 9495−9503